1446
doi:10.1017/S1431927621005353
Microsc. Microanal. 27 (Suppl 1), 2021

A robust technique to image all elements in $LiNiO_2$ cathode active material by 4D-STEM

Shamail Ahmed[1], Anuj Pokle[2], Jürgen Belz[3], Matteo Bianchini[4], Andreas Beyer[5], Jürgen Janek[6] and Kerstin Volz[5]

[1]STRL, University of Marburg, United States, [2]Materials Science Center (WZMW) and Department of Physics, Philipps-Universität Marburg, Hans Meerwein Strasse, 35032 Marburg, Germany, United States, [3]STRL, University of Marburg, Germany, [4]BASF SE, United States, [5]Materials Science Centre and Department of Physics, Philipps University Marburg, Hans-Meerwein-Straße 6, Marburg, 35032, Germany, Germany, [6]Institute of Physical Chemistry & Center for Materials Research, Justus-Liebig-University, Heinrich-Buff-Ring 17, 35392 Giessen, Germany, United States

The current demand for energy storage materials has brought a lot of interest in the scientific community to characterize these materials at the nanoscale. Lithium-ion-containing cathode-active materials (CAM), particularly layered CAMs, are of great importance in this research field. The imaging of light elements like lithium and oxygen, together with heavy elements like nickel, manganese, and cobalt, is, however, not trivial. Electron microscopy-based techniques like ptychography, using four-dimensional (4D) scanning transmission electron microscopy (STEM),[1] and focus-series reconstruction in transmission electron microscopy (TEM),[2] have stringent sample thickness requirements and require extensive image post-processing. However, it has been shown by image simulations that ABF (annular bright field) imaging in STEM is capable of imaging lithium in different compounds.[3] In addition to the imaging-related challenges, the sample preparation for a real-life sample, like secondary particles CAMs consisting of densely packed primary particles, is quite demanding. Also, it is not always possible to find the suitable crystal orientation for imaging all elements in the material due to its polycrystalline nature and its radiation sensitivity. For example, in layered CAMs, $LiCoO_2$, Nickel-Cobalt-Manganese (NCM), etc., most of the work - at atomic resolution - has been carried out in < 100 > zone axis. Although the imaging of all elements in the structure, including lithium and oxygen, is still not trivial in this zone axis, the imaging of all elements in the second most suited zone axis in this material, i.e. [210], is even more challenging because of a significant increase in interatomic distances along the electron beam direction and a significant reduction in spatial atomic distances in the STEM projection. We used -ABF (inner detector angle = 8 mrad and outer detector angle 16 mrad) to image Li in [100] zone axis at 200 kV acceleration voltage using 15.07 mrad convergence semi-angle (α).[4] However, with a conventional selection of inner and outer detector angles for ABF (i.e., $\alpha/2$ and α respectively), it is impossible to image Li in the [210] zone axis.

In this study, STEM contrast simulations have been carried out for $LiNiO_2$ in [210] zone axis up to 50 nm specimen thickness for a microscope operating at 200 kV acceleration voltage and a probe having different convergence semi-angles (from 9 mrad to 30 mrad). We measured the peak intensities from the atomic positions of Li, O, and Ni with respect to scattering angles and thickness. We subtracted background intensities from them at each scattering angle and thickness. The background is selected to be the position between two consecutive Li atomic positions. Then we plotted the negative of these values on the scattering angles vs. thickness contour-plots. Figure 1 exemplarily shows contour plots for Li, O, and Ni (at C_s = 2 μm and Δf = 0 nm) for 15 mrad and 25 mrad convergence semi-angles. The constructive and

destructive regimes for light elements, particularly Li, don't change significantly with increasing convergence semi-angle. The highest contrast from all elements in the structure decreases with increasing convergence semi-angle, which can be attributed to the better s-state coupling at lower convergence semi-angles. Our simulations suggest 15 mrad to be a decent choice for convergence semi-angle that gives good contrast together with adequate resolution in the ABF regime in this case. Reducing the convergence semi-angle from this value reduces the resolution, while increasing the value improves the resolution at the expense of contrast from light elements. The optimum inner and outer detector angles required to achieve the highest contrast from light elements at α=15 mrad in the ABF regime are found to be from 13 mrad and 15 mrad, respectively. A further contrast enhancement from light elements is achieved by subtracting the bright field (BF) image from the *optimized* ABF image to form the *optimized* eABF image.[5] We selected the inner and outer detector angles to be 0 mrad and 8 mrad for BF, respectively.

In order to verify the proposed imaging conditions (from the contrast simulations), a TEM sample has been prepared using a focused ion beam and low energy Ar-ion milling from a realistic $LiNiO_2$ CAM secondary particle, and 4D data sets have been taken using a pixelated (pnCCD) detector[4]. We applied the optimum imaging parameters as were suggested by the simulations. We show (experimentally) that it is possible to visualize all elements in the [210] zone axis by optimizing the parameters in the ABF regime, as shown in Figure 2. This method can, of course, also be applied to other materials systems, which contain elements with a large atomic number difference, as well.

https://doi.org/10.1017/S1431927621005353 Published online by Cambridge University Press

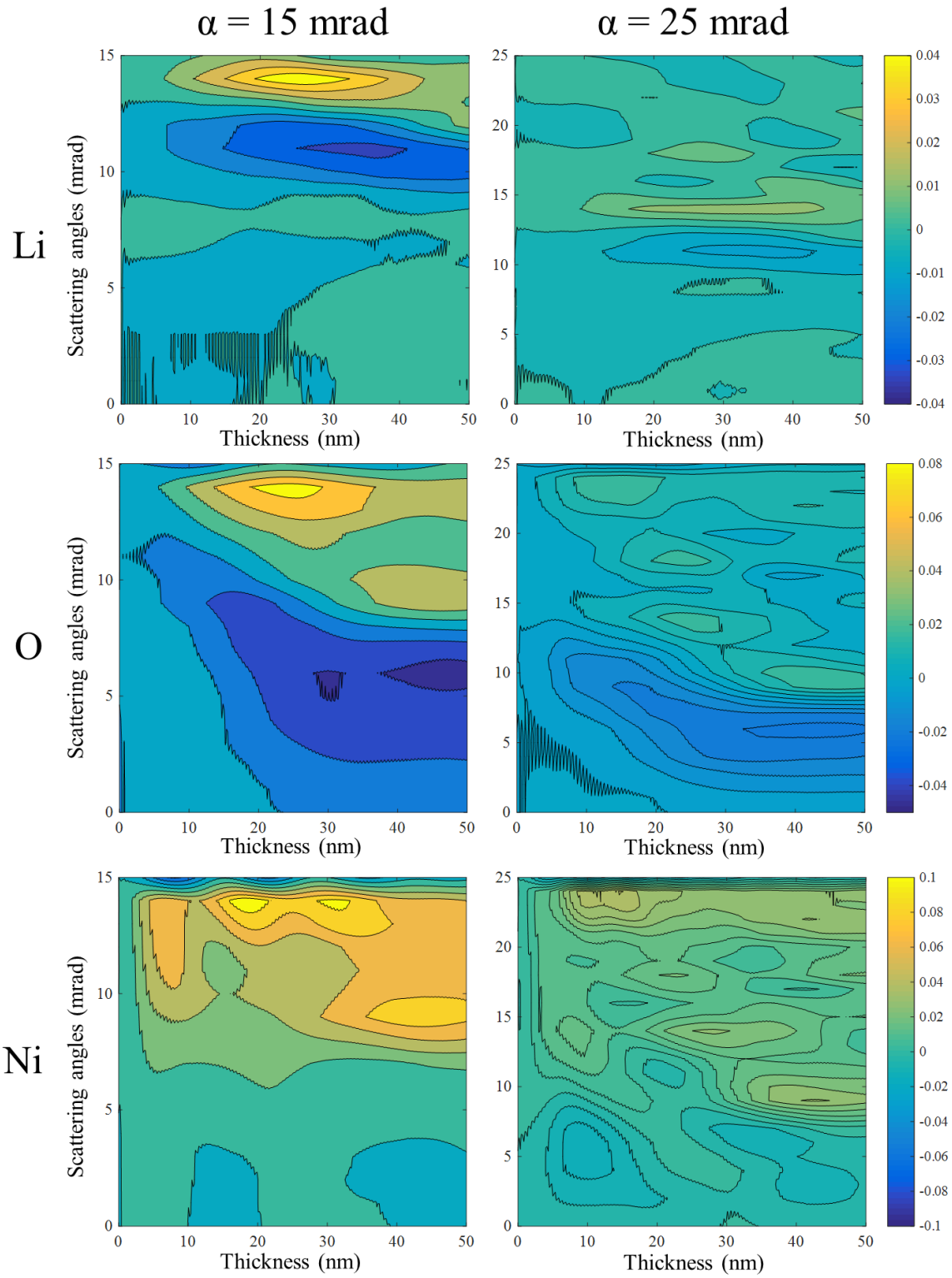

Figure 1. Figure 1: Scattering angle vs. thickness contour-plots for Li, O, and Ni atomic positions against the background-position. The first, second, and third rows show plots for Li, O, and Ni, respectively. On the right of the plots are the colobars for the contour plots in rows. The plots in the first and the second are columns at 15 mrad and 25 mrad convergence semi-angles, respectively.

https://doi.org/10.1017/S1431927621005353 Published online by Cambridge University Press

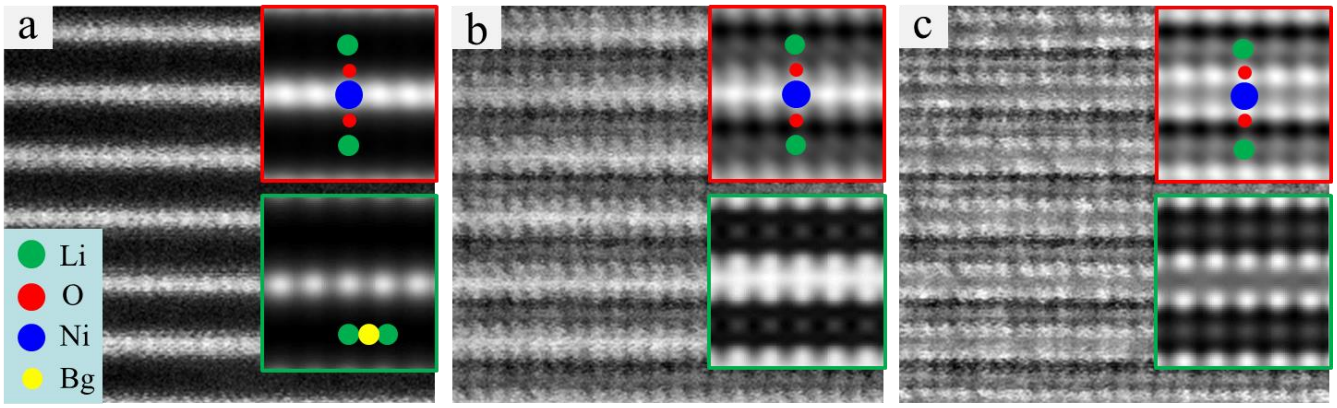

Figure 2. Figure 2: Experimental (a) high angle annular dark-field (HAADF), (b) optimized -ABF, and (c) optimized -eABF images at 20 nm sample thickness and convergence semi-angle of 15.07 mrad. The insets marked with the squares of red color show the average image from comparatively large field-of-view images. The insets marked with the squares of green color in (a, b & c) show simulated HAADF, simulated optimized -ABF images, and simulated optimized -eABF images. Green, red, blue, and yellow color circles mark Li, O, and Ni's atomic positions and background-position (Bg).

References

(1) Lozano, J. G.; Martinez, G. T.; Jin, L.; Nellist, P. D.; Bruce, P. G. Low-Dose Aberration-Free Imaging of Li-Rich Cathode Materials at Various States of Charge Using Electron Ptychography. *Nano Lett.* **2018**. https://doi.org/10.1021/acs.nanolett.8b02718.

(2) Shao-Horn, Y.; Croguennec, L.; Delmas, C.; Nelson, E. C.; O'Keefe, M. A. Atomic Resolution of Lithium Ions in LiCoO2. *Nat. Mater.* **2003**, *2* (7), 464–467. https://doi.org/10.1038/nmat922.

(3) Findlay, S. D.; Lugg, N. R.; Shibata, N.; Allen, L. J.; Ikuhara, Y. Prospects for Lithium Imaging Using Annular Bright Field Scanning Transmission Electron Microscopy: A Theoretical Study. *Ultramicroscopy* **2011**, *111* (8), 1144–1154. https://doi.org/10.1016/j.ultramic.2011.03.005.

(4) Ahmed, S.; Bianchini, M.; Pokle, A.; Munde, M. S.; Hartmann, P.; Brezesinski, T.; Beyer, A.; Janek, J.; Volz, K. Visualization of Light Elements Using 4D STEM: The Layered-to-Rock Salt Phase Transition in LiNiO2 Cathode Material. *Adv. Energy Mater.* **2020**, *10* (25), 2001026. https://doi.org/10.1002/aenm.202001026.

(5) Findlay, S. D.; Kohno, Y.; Cardamone, L. A.; Ikuhara, Y.; Shibata, N. Enhanced Light Element Imaging in Atomic Resolution Scanning Transmission Electron Microscopy. *Ultramicroscopy* **2014**, *136*, 31–41. https://doi.org/10.1016/j.ultramic.2013.07.019.

(6) We acknowledge the funding from BMBF (Bundesministerium für Bildung und Forschung) in the framework of the FESTBATT competence cluster project 03XP0176C.